Superconductivity in simple elemental solids—a computational study of boron-doped diamond and high pressure phases of Li and Si

2005 J. Phys.: Condens. Matter 17 S911

(http://iopscience.iop.org/0953-8984/17/11/023)

INSTITUTE OF PHYSICS PUBLISHING JOURNAL OF PHYSICS: CONDENSED MATTER

J. Phys.: Condens. Matter **17** (2005) S911–S920 doi:10.1088/0953-8984/17/11/023

Superconductivity in simple elemental solids—a computational study of boron-doped diamond and high pressure phases of Li and Si

John S Tse[1], Yanming Ma[2] and H M Tutuncu[3]

[1] Department of Physics and Engineering Physics, University of Saskatchewan, Saskatoon, S7N 5A2, Canada
[2] National Laboratory of Superhard Materials, Jilin University, Chang Chun 130012, People's Republic of China
[3] Department of Physics, University of Sakarya, 54187 Sakarya, Turkey

Received 5 January 2005
Published 4 March 2005
Online at stacks.iop.org/JPhysCM/17/S911

Abstract

The superconducting phase of several elemental solids under ambient (p-doped diamond) and high pressure conditions (face-centred cubic phases of Li and Si–V) have been studied with the linear response method. The computed superconducting temperatures, based on the weak coupling Bardeen–Cooper–Schrieffer theory, are found to be in good agreement with experiments. Analysis of the electronic structure and phonon band structures shows that changes in the chemical bonding are responsible for the strong electron–phonon coupling. In boron-doped diamond, the Jahn–Teller effect is shown to be the dominant factor. For high pressure FCC Li and Si–V, rehybridization has led to the redistribution of valence electrons into the interstitial space and weakened the covalent interactions that helped to enhance the electron–phonon coupling.

(Some figures in this article are in colour only in the electronic version)

1. Introduction

The observation of superconducting phases in otherwise normal solids at high pressure is not a new phenomenon. Recent advances in instrumentation and diamond anvil cell technologies have greatly expanded the pressure range and allowed the characterization of superconductivity under extreme conditions. These investigations, however, still produced some pleasant surprises [1]. For example, elemental Li in the face-centred cubic (FCC) phase, which is stable between 7.5 and 39 GPa, was found to be superconducting with very high critical temperature, reaching almost 20 K at 48 GPa [2–4]. On the other hand, ε-Fe was found to be superconducting even though it is ferromagnetic [5]. Superconductivity states at high pressure have also been reported for insulators under ambient conditions such as the molecular solid of boron [6], oxygen [7], sulfur [8] and even ionic CsI [9]. More recently, although not

at high pressure, heavily boron-doped diamond was also found to be a superconductor [10]. The superconductivity in these systems is generally rationalized within the framework of the weak coupling Bardeen–Cooper–Schrieffer (BCS) theory [11]. In the BCS model, electrons mediated by suitable phonon modes are paired in the momentum space. Several suggestions exploring the nature of the mechanism of electron–phonon coupling to real space physical models such as the electronic band structure [12] and/or to vibronic coupling in solids [13] have been made recently. The seemingly ubiquitous existence of superconductivity states for elemental solids at high pressure [1] with fairly simple crystal structures offers an opportunity to perform a systematic theoretical investigation on possible relationships between the structure and the nature of chemical bonding with superconductivity. In this paper, we first report the effects of Jahn–Teller distortion on the large phonon linewidth in boron-doped diamond [10]. The cause for the high superconducting temperature in FCC Li [2] will then be described and finally we revisit the well-characterized superconducting high pressure silicon (Si V) phase [14, 15] to reveal unique features in the chemical bond and the phonon band structure.

2. Computational details

All calculations reported in this study were performed with the pseudopotential plane wave method. Tight pseudopotentials in the Troullier–Martin form appropriate for describing electronic structure at high pressure were constructed. Linear response theory was used in the calculations of the phonon band structures and the electronic phonon coupling parameters. All calculations were performed with the PWSCF code [16]. The theory and computational methods employed here have been described in a recent review [17]. All calculations were checked against convergence in the plane wave energy cut-off and in the k-point sampling scheme.

The linewidth of the phonon mode (qj) arising from electron–phonon interaction will be used extensively in this paper to assist the analysis of the numerical results. The phonon linewidth is defined as [17, 18]

$$\gamma_{qj} = 2\pi\omega_{qj} \sum_{nm} \int \frac{\mathrm{d}^3k}{\Omega_{\mathrm{BZ}}} |g^j_{kn,k+qm}|^2 \delta(\varepsilon_{kn})\delta(\varepsilon_{k+qm}), \tag{1}$$

where the integral is over the Brillouin zone (BZ), ε_{kn} are the energy bands measured with respect to the Fermi level at point k, and Ω_{BZ} is the volume of the BZ. The matrix element

$$g^j_{kn,k+qm} = \sqrt{\frac{\hbar}{2M\omega_{qj}}} \langle kn| \frac{\delta V}{\delta u_{qj}} |k+qm\rangle, \tag{2}$$

where u_{qj} is the amplitude of the displacement of the phonon j of wavevector q, M is the atomic mass, and V is the Kohn–Sham potential. The electron–phonon coupling constant λ_{qj} for mode j at wavevector q is defined as $\lambda_{qj} = \gamma_{qj}/\pi\hbar N_{\mathrm{F}}\omega^2_{qj}$ where N_{F} is the electron density of states per atom and spin at the Fermi level ε_{F}.

The electron–phonon mass enhancement parameter λ is defined as the first reciprocal moment of the spectral function $\alpha 2F(\omega)$ [17, 18],

$$\lambda = 2\int_0^\infty \frac{\alpha^2 F(\omega)}{\omega}\,\mathrm{d}\omega \approx \sum_{qj} \lambda_{qj} w(q), \tag{3}$$

where $w(q)$ is the weight of a q point in the first BZ.

In actual computations the δ functions in equation (1) are replaced with Gaussians with appropriately chosen broadening parameters (σ) that approximate the zero limit as σ approaches zero.

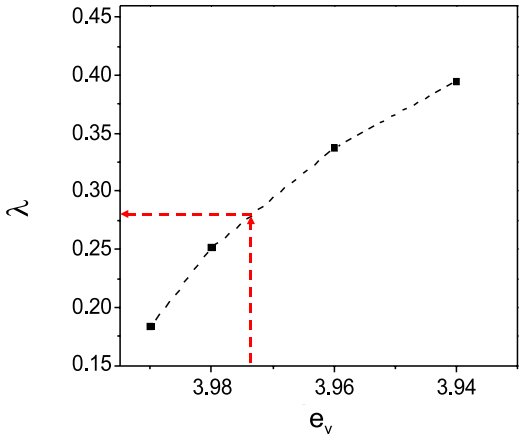

Figure 1. The theoretical electron–phonon coupling parameter λ as a function of the number of effective valence electrons (e_v) on the carbon atom in boron-doped diamond. The arrows indicate the e_v corresponding to the experimental boron concentration of 4.6×10^{21} cm^{-3} [10] and the predicted λ.

3. Results and discussion

3.1. The Jahn–Teller effect and superconductivity in boron-doped diamond

Electrical transport studies have shown that diamond (p-)doped with boron (B) at concentrations (n) $\approx 10^{17}$–10^{19} cm^{-3} is semiconducting. On increasing the B concentration to $\geqslant 10^{20}$–10^{21} cm^{-3}, doped diamond becomes metallic. More recently it was discovered that heavily doped diamond films with B concentration of $>10^{21}$ cm^{-3} are superconducting with transition temperatures of ∼4 K [10] and remain superconducting in magnetic fields of more than 3.5 T. We investigated the origin of superconductivity in the p-type diamond using *ab initio* linear response theory employing the virtual crystal approximation (VCA) [19] to mimic the hole state (p-doped) created when a small amount of B was incorporated substitutionally into the diamond. This approximation assumes implicitly that the holes created by doping are not localized but delocalized over the crystal. Since the B doping concentration is rather low, this seems to be an appropriate conjecture. More importantly, calculations reproduced correctly the observed increase of lattice constant with increasing B doping and also on the change in the Hall coefficient with B concentration. Details of the results will be presented in a forthcoming paper [20].

The theoretical electron–phonon coupling parameter (λ) as a function of the effective valence electron concentration per carbon atom (e_v) is summarized in figure 1. At the estimated experimental doped B concentration of 4.6×10^{21} cm^{-3} [10], the measured critical temperature (T_c) is 2.3 K. Using the McMillan formula, $T_c = (\theta_D/1.45)\exp(-1.04(1+\lambda)\lambda)$ [21] with a Debye temperature $\theta_D = 1860$ K [10], an electron–phonon coupling parameter of ∼0.2 was obtained. The experimental B concentration can be converted to an effective valence electron ($e_v \approx 3.974$). As shown in figure 1, the corresponding theoretical λ of ∼0.27 is in reasonable agreement with the value derived from experiment [10].

The phonon band structure of pure diamond and B-doped diamond at ($e_v = 3.98$ or $n \sim 3.6 \times 10^{21}$ cm^{-3}) is shown in figure 2. The dominant contribution to the electron–phonon coupling is associated with the softening of the optical mode at the zone centre (Γ). It is interesting to compare the calculated spectral function ($\alpha^2 F(\omega)$) with the experimental

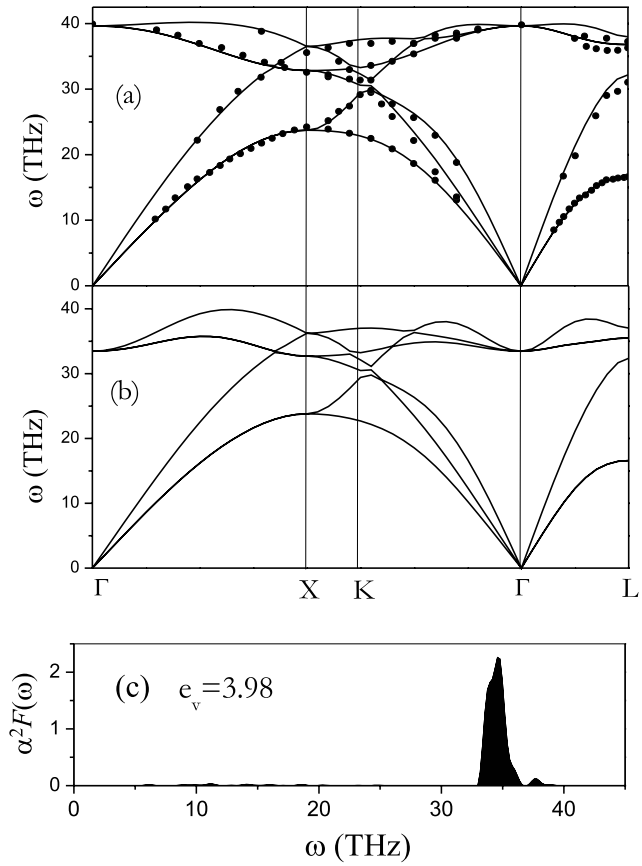

Figure 2. A comparison of theoretical and experimental phonon band structure for pure diamond under ambient conditions. (b) The calculated phonon band structure and (c) the spectral function for p-doped diamond at $e_v = 3.98$.

Raman spectrum. In the spectral function, a weak feature was observed 38 THz (1267 cm^{-1}) and a strong band at 34 THz (1167 cm^{-1}) with a width of ∼3 THz (100 cm^{-1}). These features correspond very well with the observed weak band at 1300 cm^{-1} and the broad band with a half-width of ∼100 cm^{-1} centred at 1170 cm^{-1} in the Raman spectrum [10]. Therefore, the observed broad Raman band may be the combined result of disorderings created by the boron doping and also an indication of the very large phonon linewidth due to strong electron–phonon couplings.

The origin of the large electron–phonon coupling is the consequence of a very large vibronic coupling—a strong coupling between electronic and vibrational states [13]. The highest filled band in pure diamond is the majority C 2p triply degenerate t_{1u} crystal orbital at the zone centre. The creation of hole by replacing C with B (p doping) is equivalent to the removal of electrons from this band. As a result, a spontaneous distortion must occur to lower the symmetry in order to remove the degeneracy and lower the total energy of the system. This is analogous to the Jahn–Teller (JT) effect for a molecule in an electronically degenerate state [21]. The Jahn–Teller distortion can be static or dynamic. In the case of B-doped diamond the overall crystal symmetry was preserved. Therefore rather than there being static distortion of the local symmetry around the carbon atom, the vibrational states coupled dynamically with

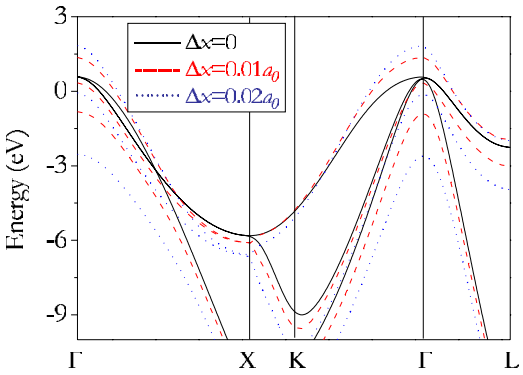

Figure 3. Calculated band structures for p-doped diamond at $e_v = 3.98$ with displacement along one of the triply degenerate t_{1u} vibration modes. The magnitude of the atom displacement is indicated in the inset.

the electronic state. The strength of vibronic coupling may be estimated by computing the change in the electronic band structure from the displacement of the carbon atoms along the t_{1u} vibrational mode. As shown in figure 3, a small distortion (e.g. displacement of ∼0.03 Å) resulted in large changes in the profile of the electronic bands near the Fermi surface. More importantly, it is shown that the vibronic effect is strongest at Γ where the degeneracy of the band is broken and opens a 'gap' of almost 3 eV. The change in the band structure is evidently much weaker at other symmetry points. This observation is in good accord with phonon linewidth calculations which show that the main contribution to the electron–phonon coupling is the vibration near the Γ point. The results presented here suggest the concept of the 'chemistry of vibronic coupling' may be transferred to solid state materials [13].

3.2. FCC Li and the role of soft phonon modes

The ambient body-centred cubic (BCC) phase of Li is not superconducting. At 7.5 GPa, BCC Li transforms into the FCC structure [25]. The observation of superconductivity in the high pressure FCC phase of Li [2–4] came as a surprise, even though telltale signs of possible superconductivity had already been reported in the literature [23]. Li is the simplest metallic element in the periodic table and with one valence electron it is not expected to be a good candidate for showing superconductivity [24]. An early theoretical calculation [25] based on the rigid muffin approximation (RMT) and employing a 'normal' Coulomb coupling constant ($\mu^* = 0.13$) predicted that the FCC phase of Li is superconducting and should reach a critical temperature $T_c \sim 40$–80 K. The predicted T_c is too high, by a factor of ∼4, from the subsequent experimental measurements [2–4]. To understand the origin of the superconductivity, we have calculated the lattice dynamics, phonon linewidth and the electron–phonon coupling parameter λ of the FCC Li phase as a function of pressure.

The calculated λs are compared with previous RMT results in figure 4. The predicted trend of increasing λ with decreasing volume (or increasing pressure) is the same. However, the discrepancy in the calculated magnitude of λ is fairly large and with the RMT approximation consistently higher than the present linear response calculations. To obtain numerical agreement with experimental T_c using the McMillan equation, a much larger and pressure dependent $\mu^* \sim 0.23$–0.26 had to be used. These μ^* values are much larger than the 'normal' value of ∼0.1–0.15 but are consistent with an elaborate calculation of the Coulomb pseudopotential for direct electron–electron repulsions in the BCC phase of Li [26]. The

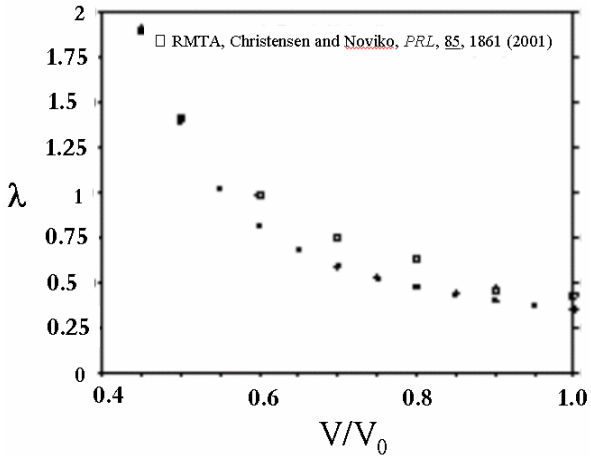

Figure 4. The theoretical electron–phonon parameter λ as a function of the volume of FCC Li.

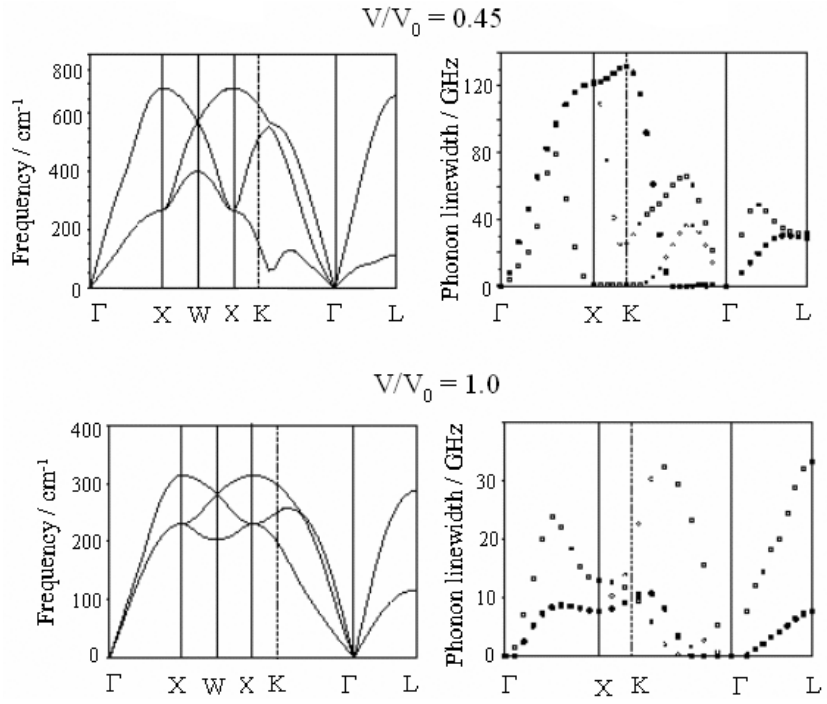

Figure 5. The theoretical phonon band structure (left panel) and phonon linewidth for FCC Li at $V/V_0 = 1.0$ (bottom) and $V/V_0 = 0.45$ (top). Note that, at $V/V_0 = 1.0$, the linewidths for the LA phonons are larger than those for the TA modes, but the trend is reversed at higher pressure.

multiple-band contribution to the electron–electron interaction in the metallic case is obviously very important and cannot be easily described using a simple model.

Inspection of the phonon band structure reveals that at high pressure the transverse (TA) phonon branch along the X → K softens substantially (figure 5). The softening is accompanied by increasingly larger phonon linewidth for the TA phonons along the same symmetry direction

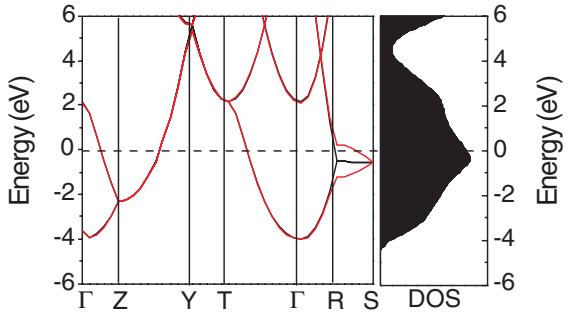

Figure 6. Left: calculated electronic band structures for FCC Li (unit cell parameter = 3.1856 Å) with displacement along the X phonon mode (black full line = 0.0, red dashed line = 0.0656 Å). Right: the electronic density of states (DOS) for undistorted Li in the FCC and *Cmcm* crystal symmetry. (Note that the differences between the two calculations are indistinguishable.)

(see figure 5 $V/V_0 = 0.45$). Since the electron–phonon parameter is directly proportional to the phonon linewidth and inversely proportional to the corresponding vibrational frequency, a combination of these two effects resulted in a large phonon–electron coupling parameter. To investigate the effects of the soft TA phonon modes on the electronic band structure, frozen phonon calculations were performed by displacing the appropriate atoms along the X point phonon normal coordinates. To incorporate the X point phonon, it is necessary to double the unit cell and reduce the crystal symmetry from cubic to orthorhombic *Cmcm* [27]. The results of the calculations are shown in figure 6. In the undistorted structure a flat band (non-dispersive) along S $\rightarrow$ R was observed. This band is responsible for the maximum observed in the electron density of states and is related to the band in the vicinity of the L point in the original FCC unit cell. It is clear from the figure that the electronic bands along S $\rightarrow$ R distort significantly following the displacement along the X phonon mode, while there is little change in the other directions. The otherwise relatively flat band along S $\rightarrow$ R is significantly perturbed by the phonon vibration and splits into two bands opening a large gap when one of the bands crosses the Fermi surface. This behaviour is similar to the JT effect on doped diamond discussed above (*vide supra*). Therefore, the softening of the TA branch near X and along X $\rightarrow$ K induced a change in the band structure resulting in large charge fluctuation and strong electron–phonon coupling.

3.3. Si V, a one-dimensional covalent solid

The electronic structure and superconductivity in Si V, a high pressure phase of Si stable between 16 and 38 GPa, are well studied [14, 15]. Some of the pioneering electronic calculations on the band structure, lattice dynamics and electron–phonon coupling [15] had been focused on this material. Recently, we presented a systematic investigation on the nature of chemical bond in the successive high pressure phases of Si using a real space description [28]. In particular, the concept of electron localization function (ELF) [29] was used to analyse the electron distribution and to characterize the bonding. The ELF is a convenient indicator for the identification of chemical bonding in sp compounds. Usually, the ELF has a value between 0.5 and 1.0. In general, the higher the ELF the higher the probability of electron localization and, therefore, the higher the degree of 'covalency'. When ELF = 0.5, the valence electrons behave like free electron gas. The essence of the ELF analysis of various phases of high pressure silicon is shown in figure 7. Using ELF = 0.8 as a reference, it can be seen that the

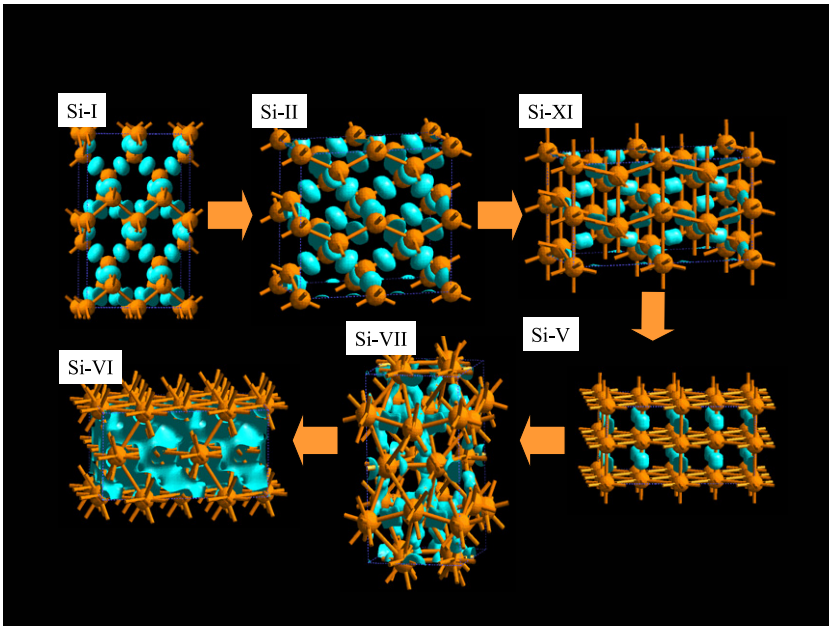

Figure 7. A 3D representation of the electron localization function (ELF) for the high pressure phases of Si. An ELF surface contour of 0.8 was used for Si I, Si II, Si IX and Si V to illustrate the reduction in the 'bonding' dimensionality. A smaller ELF value of 0.7 was used for Si VII, indicating the diminishing tendency for electron localization. Si VI is fully metallic and therefore an ELF contour value of 0.5 was used.

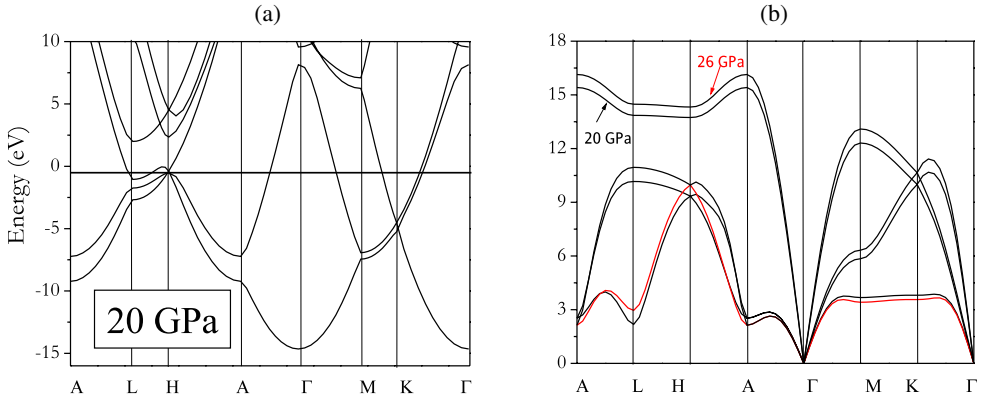

Figure 8. The theoretical electronic band structure for Si V at 20 GPa (a) and the phonon band structure at 20 and 26 GPa (b).

dimensionality of the 'covalent' bonding network in Si decreases gradually with increasing pressure and leads to several structural transformations. From a chemical perspective, the covalent bonding network changes from sp^3 in Si I and Si II to sp^2 in Si XI, to sp in Si V, eventually becoming metallic in Si VI and Si VII (ELF = 0.5). The change in hybridization is accompanied by the promotion of Si 3p valence electrons into more diffuse Si 3d orbitals, thus increasing the electron mobility and the metallicity. As shown in figure 7, in Si V the chemical

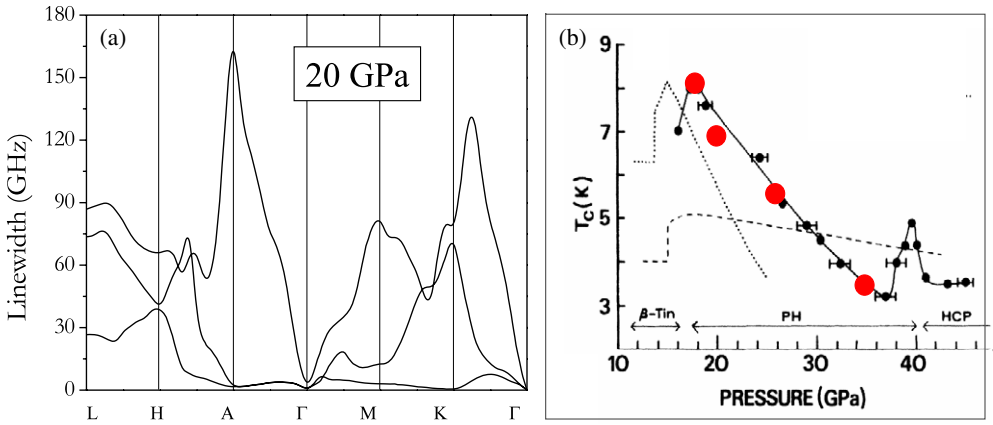

Figure 9. (a) The theoretical phonon linewidth for Si V at 20 GPa. (b) A comparison of the experimental (taken from [14]) and predicted (large red circle) critical temperature T_c for Si V.

bonds are between chains of Si atoms perpendicular to the hexagonal plane. The electronic band structure calculated at 20 GPa (figure 8(a)) clearly shows strongly dispersive parabolic bands cutting the Fermi surface in the A $\rightarrow$ Γ $\rightarrow$ M and K $\rightarrow$ Γ directions. On the other hand, there are relatively flat bands in the L $\rightarrow$ H case. The profiles of the band structures remain similar even when the pressure is increased to 35 GPa. The phonon band structures calculated at 20 and 26 GPa are compared in figure 8(b). With increasing pressure the frequency of the longitudinal transverse (LA) phonon also increases. In contrast, the frequencies of the TA branches along the A $\rightarrow$ Γ $\rightarrow$ M $\rightarrow$ K $\rightarrow$ Γ directions decrease slightly with pressure. The calculated phonon linewidths at 20 GPa are shown in figure 9(a). The LA phonons have the largest linewidth. However, their contribution to the electron–phonon coupling parameter is weighed down somewhat by the higher vibrational frequencies. On the other hand, a TA phonon branch from Γ $\rightarrow$ M $\rightarrow$ K $\rightarrow$ Γ also has relatively large phonon linewidth. In view of the lower frequencies of the TA phonons, these modes also made significant contributions to the electron–phonon parameter. The electron–phonon coupling parameter for Si V is found to decrease with pressure. Using a constant $\mu^* = 0.12$, the experimental critical temperature and the pressure dependence are well reproduced (figure 9(b)).

4. Summary

The theoretical results presented here show that the BCS model is valid for the rationalization of the superconductivity in high pressure elemental solids. There are some common features in the electronic band structure that are shared by the systems studied here. For example, it is shown that the strong vibronic coupling in p-doped diamond and FCC Li which led to large charge fluctuations may be related to large electron–phonon couplings. According to a recent proposal [12] which is loosely related to the itinerant electron versus local pair model [30], a necessary condition for possible superconductivity is the simultaneous occurrence of dispersive band(s) which cross(es) the Fermi surface and non-dispersive bands located near the Fermi surface. Apparently this two-band scenario [12] is satisfied for all the systems studied here.

References

[1] Ashcroft N W 2002 *Nature* **419** 569
[2] Shimizu K, Ishikawa H, Takao D, Yagi T and Amaya K 2002 *Nature* **416** 597

[3] Struzhkin V V, Eremets M I, Gan W, Mao H K and Hemley R J 2002 *Science* **298** 1213
[4] Deemyad S and Schilling J S 2003 *Phys. Rev. Lett.* **91** 167001
[5] Shimizu K, Kimura T, Furomoto S, Takeda K, Kontani K, Onuki Y and Amaya K 2002 *Nature* **412** 3196
[6] Eremets M I, Struzhkin V V, Mao H-K and Hemley R J 2001 *Science* **293** 272
[7] Shimizu K, Suhara K, Ikumo M, Eremets M I and Amaya K 1998 *Nature* **393** 767
[8] Struzhkin V V, Hemley R J, Mao H-K and Timofeev Y A 1997 *Nature* **390** 382
[9] Eremets M I, Shimizu K, Kobayashi T C and Amaya K 1998 *Science* **281** 1333
[10] Ekimov E A, Sidorov V A, Bauer E D, Mel'nik N N, Curre M J, Thompson J D and Stishov S M 2004 *Nature* **428** 542
[11] Bardeen J, Cooper L N and Schrieffer J R 1957 *Phys. Rev.* **108** 1175
[12] Simon A 1997 *Agnew. Chem. Int. Edn Engl.* **36** 1788
[13] Grochala W, Hoffmann R and Edwards P P 2003 *Chem. Eur. J.* **9** 575
[14] Chang K J, Dacorogna M M, Cohen M L, Mignot J M, Chouteau G and Martinez G 1985 *Phys. Rev. Lett.* **54** 2375
[15] Dacorogna M M, Chang K J and Cohen M L 1985 *Phys. Rev.* B **32** 1853
Chang K J and Cohen M L 1984 *Phys. Rev.* B **30** 5376
[16] Baroni S, Dal Corso A, de Gironcoli S and Giannozzi P http://www.pwscf.org
[17] Baroni S, de Gironcoli S, Dal Corso A and Giannozzi P 2001 *Rev. Mod. Phys.* **73** 515
[18] Savrasov S Y 1996 *Phys. Rev.* B **54** 16470
[19] Nordheim L 1931 *Ann. Phys., Lpz.* **9** 607
[20] Ma Y, Tse J S and Klug D D 2005 *Phys. Rev. Lett.* submitted
[21] McMillan W L 1968 *Phys. Rev.* **167** 331
[22] Mathias B T 1955 *Phys. Rev.* **97** 74
[23] Jahn J and Teller E 1937 *Proc. R. Soc.* A **161** 220
[24] Lin T H and Dunn R J 1986 *Phys. Rev.* B **33** 807
[25] Christensen N E and Novikov D L 2001 *Phys. Rev. Lett.* **86** 1861
[26] Richardson C F and Ashcroft N W 1997 *Phys. Rev.* B **55** 15130
[27] For details see: http://cst-www.nrl.navy.mil/~mehl/phonons/fcc
[28] Tse J S, Ma Y and Dewhurst J K 2005 at press
[29] Edgecombe K and Becke A 1990 *J. Chem. Phys.* **92** 5397
[30] Micnas R, Ranninger J and Robaszkiewicz S 1990 *Rev. Mod. Phys.* **62** 113